Local Axon Collaterals of Area CA1 Support Spread of Epileptiform Discharges Within CA1, but Propagation is Unidirectional

R. Orman,[1] H. Von Gizycki,[2] W.W. Lytton,[1,3] and M. Stewart[1,3]*

ABSTRACT: CA3 and subiculum are hippocampal formation regions that can initiate seizure activity because each has a substantial intrinsic excitatory connectivity. We studied the intrinsic connectivity of area CA1 by exploring the spread of synchronous population discharges in ventral hippocampal slices from rats using a recording chamber that permitted multiple simultaneous extracellular recordings along all laminae of CA1. Brief single stimulus pulses were applied to stratum oriens (SO) or stratum radiatum (SR) on the CA3 side or the subicular side of CA1. In disinhibited slices, events triggered with SO or SR stimulation on the CA3-side propagated over the proximo-distal extent of CA1 with a maximal conduction velocity of 0.4 m/s, comparable with antidromic conduction velocities within CA1. By contrast, SO or SR stimuli applied on the subicular side of CA1 triggered events that did not spread "backward" toward CA3. These events are rapidly decremented in amplitude and duration. Whereas antidromic responses were largest when stimuli were applied on the subicular side of CA1, such responses were not sufficient to trigger epileptiform discharges when excitatory transmission was intact. We conclude that the unidirectional spread of epileptiform activity in area CA1 is the result of an intrinsic axon collateral system where each pyramidal cell has a proportionally larger projection toward subiculum. Although this collateral system is sparse compared with other hippocampal formation regions, its unidirectionality protects against re-entrant activation of CA3 and may be physiologically significant as a relay from proximal CA1 to distal CA1. © **2008 Wiley-Liss, Inc.**

KEY WORDS: hippocampus; trisynaptic pathway; intrinsic circuitry; seizure

INTRODUCTION

The hippocampal formation, comprising hippocampus, entorhinal cortex (EC) and subicular areas, is a collection of cortical brain regions with a variety of cell types and circuits [reviewed in (Amaral and Lavenex, 2007; Witter and Amaral, 2004)]. Two allocortical regions, dentate gyrus (DG) and Ammon's horn (CA1-CA3), are characterized by a single layer of principal neurons. The neighboring parahippocampal areas (EC, parasubiculum, presubiculum and subiculum) form the anatomical transition between hippocampus and the isocortex. The EC, parasubiculum, and presubiculum more closely resemble isocortex, having multiple distinct cell layers with stellate and pyramidal cells.

Studies of the various hippocampal formation regions have led to the widely held view that the combination of a critical density of recurrent excitatory connectivity and spontaneous activity in the some of the cells (pacemaker cells) is required for a brain region to generate seizure activity [e.g., (Heinemann, 1987; Traub et al., 1999)]. Many regions that initiate seizure activity contain an abundance of burst firing neurons and the bursting cells have even been shown to be pacemaker cells [e.g., (Miles and Wong, 1983; Jensen and Yaari, 1997; Harris and Stewart, 2001a)]. The local intrinsic connectivity in each region typically shows a concentration of local collaterals nearest the cell of origin [with some variation in axonal density (Li et al., 1994); or variations dependent on cell types (Harris et al., 2001); reviewed in (Witter and Amaral, 2004; Amaral and Lavenex, 2007)].

A combination of biological experimentation and computer simulations has been used to define the roles of the relatively dense intrinsic excitatory connectivity and cellular properties of CA3 in generating epileptiform activity [reviewed in (Traub et al., 1999)]. Briefly, population (epileptiform) bursts result from synaptic depolarization that drives dendritic calcium spiking. The event is terminated as the afterhyperpolarizing conductance (a slowly activating and inactivating calcium-dependent potassium conductance) grows to offset the intrinsic calcium current and the sustained excitatory synaptic excitation. Available GABA mediated conductances can also shape the duration of the event.

The DG and CA1 are normally resistant to seizure generation. A lack of a critical density of recurrent excitatory connectivity is the preferred explanation for why CA1 does not produce spontaneous epileptiform activity in disinhibited tissue (Traub et al., 1999). The firing properties of CA1 burst-firing pyramidal cells are different from cells in CA3 and subiculum [reviewed in (Traub et al., 1999; Spruston and McBain, 2007)], but intrinsic connectivity more than burst firing appears to be critical for the generation of synchronous population discharges since parahippocampal regions that do not contain burst firing cells can generate epileptiform discharges (Funahashi and Stewart, 1997; Funahashi et al., 1999). Differences between "heavily" interconnected and "sparsely" interconnected regions are, however, quite small. Estimates

[1] **Department of Physiology and Pharmacology, State University of New York, Downstate Medical Center, Brooklyn, New York;** [2] **Scientific & Academic Computing, State University of New York, Downstate Medical Center, Brooklyn, New York;** [3] **Department of Neurology, State University of New York, Downstate Medical Center, Brooklyn, New York**
Grant sponsor: NIH; Grant number: NS045612
*Correspondence to: Mark Stewart, Departments of Physiology & Pharmacology, and Neurology, State University of New York Downstate Medical Center, Box 31, 450 Clarkson Avenue, Brooklyn, NY 11203, USA. E-mail: mark.stewart@downstate.edu
Accepted for publication 26 April 2008
DOI 10.1002/hipo.20460
Published online in Wiley InterScience (www.interscience.wiley.com).

© *2008 WILEY-LISS, INC.*

of pyramidal cell to cell connectivity in the heavily interconnected CA3 are 2% [e.g., (Li et al., 1994)] whereas connectivity estimates are 1% [e.g., (Deuchars and Thomson, 1996)] for cells in the sparsely interconnected area CA1 [reviewed in (Traub et al., 1999; Witter and Amaral, 2004)].

The study of epileptiform activity in disinhibited brain slice preparations is a powerful tool for exploring the properties of excitatory connectivity. We sought to explore the properties of the intrinsic connectivity of area CA1 by studying the spread of synchronous population discharges along the proximo-distal axis. The goal of this study was to explore the properties of the sparse intrinsic connectivity of CA1 using a recording technology that offered numerous simultaneous recording sites along multiple lamina of CA1. The large number of electrodes available and the fact that we can directly visualize their location on the slice results in very precisely directed electrodes, and the use of field recordings has the advantage of offering a much better picture of population behavior. We set out to define basic features of the intrinsic collateral system for the spread of population events in a cytoarchitechtonically simple structure with sparse connectivity, as we did in the adjacent subiculum (Harris and Stewart, 2001a; Harris et al., 2001). We discovered asymmetrical propagation, the basis for which is instructive in refining current circuit diagrams of the hippocampus.

METHODS

All procedures were approved by the University's Animal Care and Use Committee and conform to NIH guidelines.

Slice Preparation and Maintenance

Male Sprague-Dawley albino rats (150–200 g, 3–5 weeks old) were anesthetized with halothane and decapitated. Each brain was removed from the skull, bisected, and placed briefly in ice cold artificial CSF. Thick slices of tissue (about 1–2 mm thick) were cut horizontally from the intact hemispheres with its dorsal face at about the level of the hippocampal genu. Thin slices (350–400 μm) were cut using a Leica VT1000S sectioning system (Leica, Nussloch, Germany) and transferred to a holding chamber. Final slices were simple horizontal sections (Fig. 1) trimmed with a cut perpendicular to the midline on the rostral side of area CA3 and the level of the slices corresponded to a range of about 2.6–4.6 mm above the interaural line (Paxinos and Watson, 1998). In some slices, large cuts were made to completely remove area CA3 and/or small radially-oriented cuts were made to disconnect area CA1 from surrounding regions.

From the holding chamber, single slices were placed in the MED64 chamber (Panasonic MED64, Osaka, Japan). The MED64 chamber is a 22 mm diameter well formed from a plastic ring cemented to a glass base that contains the electrodes. Conductive strips embedded in the glass base terminate in platinum-platinum black electrodes that are nearly flush with the well floor (see below). Flow is regulated such that slices are just below an interface configuration.

The perfusion solution (1 ml/min) was composed of (in mM): NaCl 125, KCl 2.5 to 5, $CaCl_2$ 1.7, $MgCl_2$ 1.2, $NaHCO_3$ 26, and glucose 10; pH = 7.4 when exposed to 95% O_2 and 5% CO_2. The temperature of the MED64 chamber was maintained at 30°C by warming the perfusate with an inline heater. The ventral horizontal slice preparation contains area CA1 and many of the surrounding areas, including: CA3, subiculum, presubiculum, and EC (Stewart, 1999; Harris and Stewart, 2001b; Kunitake et al., 2004).

Recording and Stimulating Techniques

The MED64 chamber allows simultaneous extracellular recordings from 64 electrodes (50 μm squares). Each electrode is a platinum black-plated square embedded in the floor of the recording chamber. Interelectrode distances (center to center) were 100, 150, or 300 μm. Most recordings were made with 100 or 150 μm contact spacing to concentrate electrodes within area CA1. Recording electrode impedances are 22 kΩ (at 1 kHz) and each is referred to a single set of four reference electrodes in the periphery of the chamber that are electrically tied together. The recording electrodes are arranged in an 8 × 8 array embedded on the bottom of the chamber (Fig. 1).

Brief stimulating pulses were delivered using platinum-iridium parallel bipolar stimulating electrodes (150 μm tip separation; FHC, Bowdoinham, ME) with <100 kΩ electrode impedances. Stimuli were biphasic pulses (50–100 μs in total duration) applied through constant current stimulus isolation units. The bipolar stimulating electrode was placed from the top side of the slice. The stimulating electrodes were placed in one of four locations (Fig. 1): (a) in stratum oriens on the CA3 side of CA1; (b) in stratum radiatum on the CA3 side of CA1; (c) stratum oriens on the subicular side of CA1; or (d) stratum radiatum on the subicular side of CA1. Typically two or more loci were tested in each slice. The stimulus intensity at each location was varied to compare stimulus currents across locations, to elicit comparably-sized responses at the closest electrode, and/or to explore the onset of synaptic or antidromic responses. We tested a number of orientations (e.g., parallel with anatomical laminae or perpendicular to anatomical laminae, cathode or anode "leading") for the stimulating electrodes. For analyses, we used orientations where the pair of electrodes was within a lamina, or as close to that as possible, and where the cathode was the "leading" electrode.

Data were digitized at 20 kHz per channel and stored on disk using MED64 Conductor software. Events were studied offline using MED64 Conductor software, custom LabVIEW (National Instruments, Austin, TX) programs, Microsoft EXCEL macros, and custom NEURON-based software programs.

Pharmacology

All drugs were applied to the bath by adding them to the perfusate reservoir. The concentrations given are concentrations

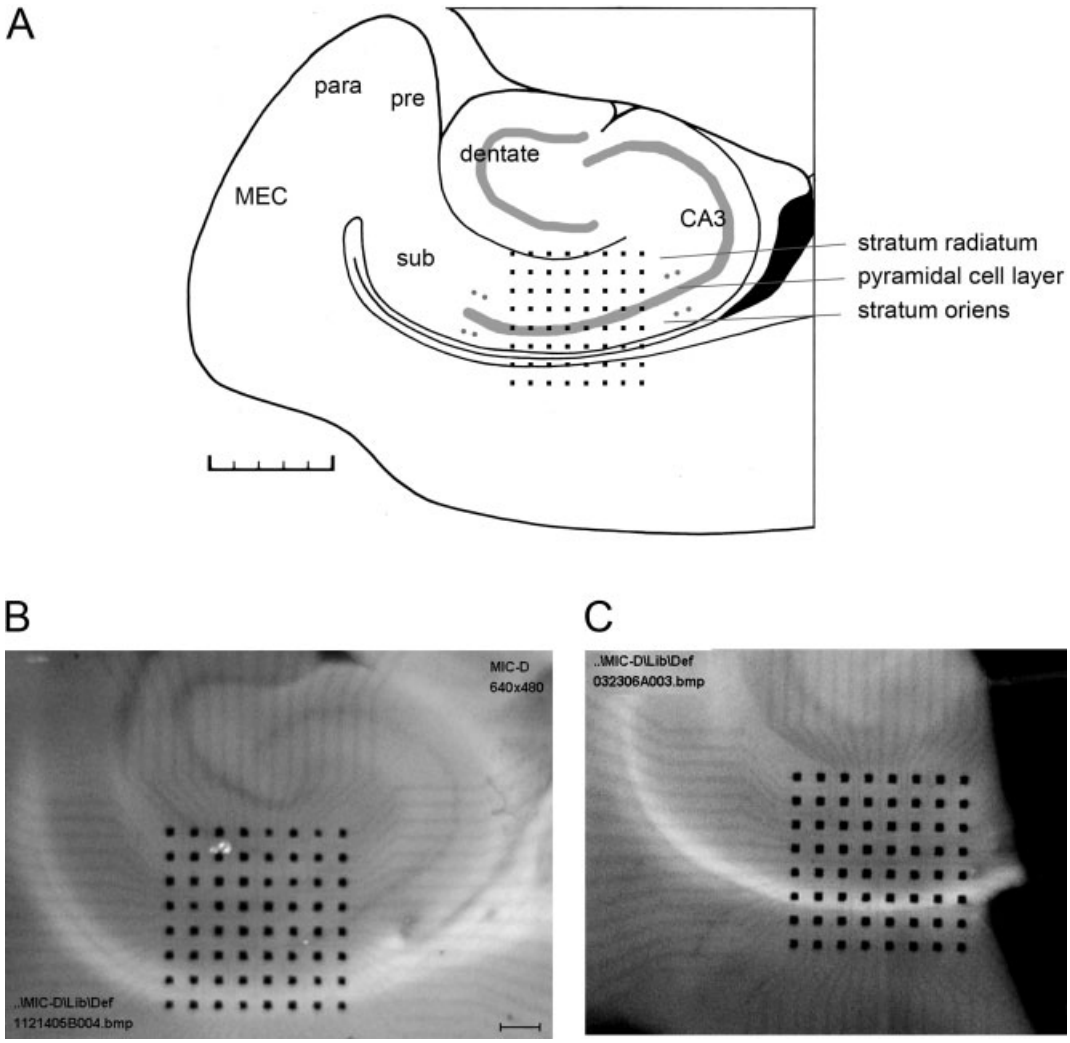

FIGURE 1. Diagram of the hippocampal slice, the recording grid electrode, and stimulating locations. A: Diagram of the ventral hippocampal slice, with major regions labeled. Note that CA1 is covered by the 8 × 8 grid elecrode and is not labeled. The location of the grid electrode (the illustration approximates the 150 μm contact spacing). Note that electrodes lie along the cell layer and cover the dendritic axis as well. Four stimulating electrode pairs are illustrated in stratum oriens and stratum radiatum on either side of the recording grid. The scale bar is 1 mm in total length. B, C: photomicrographs of a full slice (B) and a slice that has CA3 cut off (C) with 100 μ contact spacing. The image is taken by viewing through the electrode-embedded floor of the slice chamber up to the slice.

that exist in the reservoir and were achieved in the recording chamber over a period of minutes. Recordings in the presence of all drugs were taken after sufficient time for equilibration in the recording chamber. Equilibration was apparent in recordings as a change in evoked response.

Bicuculline (bicuculline methiodide, 50 μM), AP-5 (DL-(−)-2-amino-5-phosphonopentanoic acid, 40 μM), CPP (3-((RS)-2-carboxypiperazin-4-yl)-propyl-1-phosphonic acid, 20 μM), and CNQX (6-cyano-7-nitroquinoxaline-2,3-dione or 6-cyano-7-nitroquinoxaline-2,3-dione disodium, 20 μM) were obtained from Sigma (Sigma-Aldrich, St. Louis, MO). 2-hydroxysaclofen (200 μM) and some batches of CNQX and CPP were obtained from Tocris Bioscience (Ellisville, MO). Bicuculline was used to antagonize GABA-A receptors. Saclofen was used to antagonize GABA-B receptors. AP5 and CPP were used as NMDA receptor antagonists, and CNQX was used as an AMPA receptor antagonist. All slices were disinhibited with bicuculline. The combination of glutamate receptor antagonists was used to block excitatory transmission, thereby exposing antidromic responses of pyramidal cells.

Data Analysis

We chose to focus on the set of electrodes that laid directly along and/or adjacent to the cell layer so that we were well positioned to observe firing. We extracted a set of features from each sweep of each channel that included the following. (A) *Event Onset*. We took the first deflection from baseline that was due to evoked activity in either the positive or negative direction as the earliest event onset. In some recordings that were close to the stimulating electrode, the stimulus artifact made detection difficult or impossible. In a number of these cases, we used stimulus polarity reversals and comparisons of evoked responses to

responses evoked in the presence of glutamate receptor blockade to be able to identify the onset of synaptically mediated or antidromic activity. In a small number of slices, we captured spontaneous events spreading through area CA1. Onset measures in these cases are discussed in the results. (B) *Area*. We full-wave rectified responses and integrated the resulting waveform to determine the area of the response between the onset and end of each evoked response. (C) *Amplitude*. We scanned the evoked response for the maximum negativity and maximum positivity (in any order). The difference between these values was taken as the maximal peak-to-peak amplitude. The absolute value of the amplitude is reported. (D) *Total event duration*. The baseline before stimulation was always very flat. The end of the evoked response was taken as the point at which the evoked response completely returned to baseline. The difference between the endpoint and the event onset was taken as the total event duration. (E) *Early event duration*. Each event consisted of a period of firing that was followed by a slow wave. The difference between the end of firing (transition to the slow wave) and the event onset was taken as the duration of the early part. Features were extracted from each trace and features were averaged for each channel.

Statistics

Averages for particular values (e.g., magnitudes at the closest electrode position) were compared with analysis of variance (ANOVA). Values in the text are presented as means plus/minus standard errors of the mean.

Repeated measures regression was performed using general linear mixed models to predict onset, area, amplitude or duration of the response using distance as a predictor and its interaction with location (four levels: SO, SR on CA3 side and subicular side) to test if the slope of each plot of parameter with distance was dependent on stimulus location. The assessment of distance as a predictor was performed for each location by testing slopes of parameter by distance against 0. Significantly positive slopes were interpreted as an increase, significantly negative slopes were interpreted as a decrease and slopes that were not significantly different from zero were interpreted as representing an unchanging parameter as a function of distance (e.g., a response whose duration was the same at each distance). Additionally, these slopes were contrasted to assess the slope differences between the locations. The best fitting covariate structure from the general linear mixed models was used. The slope analyses were similar to, but comparisons were more robust than, the determination of Pearson product moment correlation coefficients (r).

RESULTS

We studied activity from horizontal slices taken from the ventral hippocampal formation of rats. Full slices contained DG, areas CA3 and CA1, subiculum, pre- and parasubiculum, and the EC. In a number of slices we also made knife cuts to separate area CA1 from area CA3 and/or subiculum. Recordings were made with an 8 × 8 electrode grid where at least eight electrodes laid along the cell layer of CA1. For the statistical comparisons, stimulus currents producing comparable initial responses were used. The stimulating locations used to trigger population events were in the stratum radiatum or stratum oriens on either the CA3 side of CA1 or the subicular side of CA1. The independently moveable stimulating electrode had a variable distance to the nearest grid electrode. Plots of activity as a function of distance are made using the actual distances of grid electrodes from the stimulating electrode. For analyses, we used data from slices that were stimulated from at least one proximal and one distal stimulating site.

Responses Evoked From the Proximal or Distal Side of CA1

In the presence of bicuculline to block GABA-A receptor-mediated transmission, stimuli evoked population responses that propagated from the CA3 (proximal) side of CA1 to the subicular (distal) side of CA1. Propagation in the direction toward subiculum was characterized by declines in amplitude measures (area and peak-to-peak amplitude), but stable or increasing event durations as a function of distance away from the stimulating electrode (response "broadening" – see Figs. 2 and 3). Some of these measures are plotted and compared in Figure 3 and Table 1.

Evoked population events were characterized by an initial period of population spiking followed by a late slow component that was free from spiking (Fig. 4). The slow component was not mediated by GABA-A receptor activation, nor was it mediated by GABA-B or NMDA receptor activation because all slices were studied in bicuculline and addition of saclofen, CPP, or AP5 to the bath were all without effect in reducing this late event [data not shown, see also (Funahashi and Stewart, 1998)]. Additionally, antidromic population spikes were not accompanied by similar late events suggesting minimal contributions from intrinsic ionic conductances. The late slow event is discussed further, below.

When each of the outcome measures (onset, area, amplitude, durations) was assessed using distance and location as factors in a regression model, the analysis of interest was the interaction between distance and location. In plots (Fig. 3), and for statistical comparisons of slopes (Table 1), we normalized responses by dividing each of the eight values for a given slice by the first (closest to stimulator) value from that slice. Interactions were significant for the two duration measures, early duration ($F_{3,143} = 21.4$, $P = 0.000$) and total duration ($F_{3,216} = 57$, $P = 0.000$), indicating a difference in the parameter-distance slopes across stimulus locations, but interactions were not significant for onset ($F_{3,202} = 0.9$, NS), amplitude ($F_{3,217} = 0.9$, NS), or area ($F_{3,220} = 1.9$, NS) measures. We explored the parameter-distance relations further by estimating regression parameters and assessing the differences of the slopes. Slopes differed for the duration measures but not the amplitude measures, depending on the stimulus location. Regression lines are

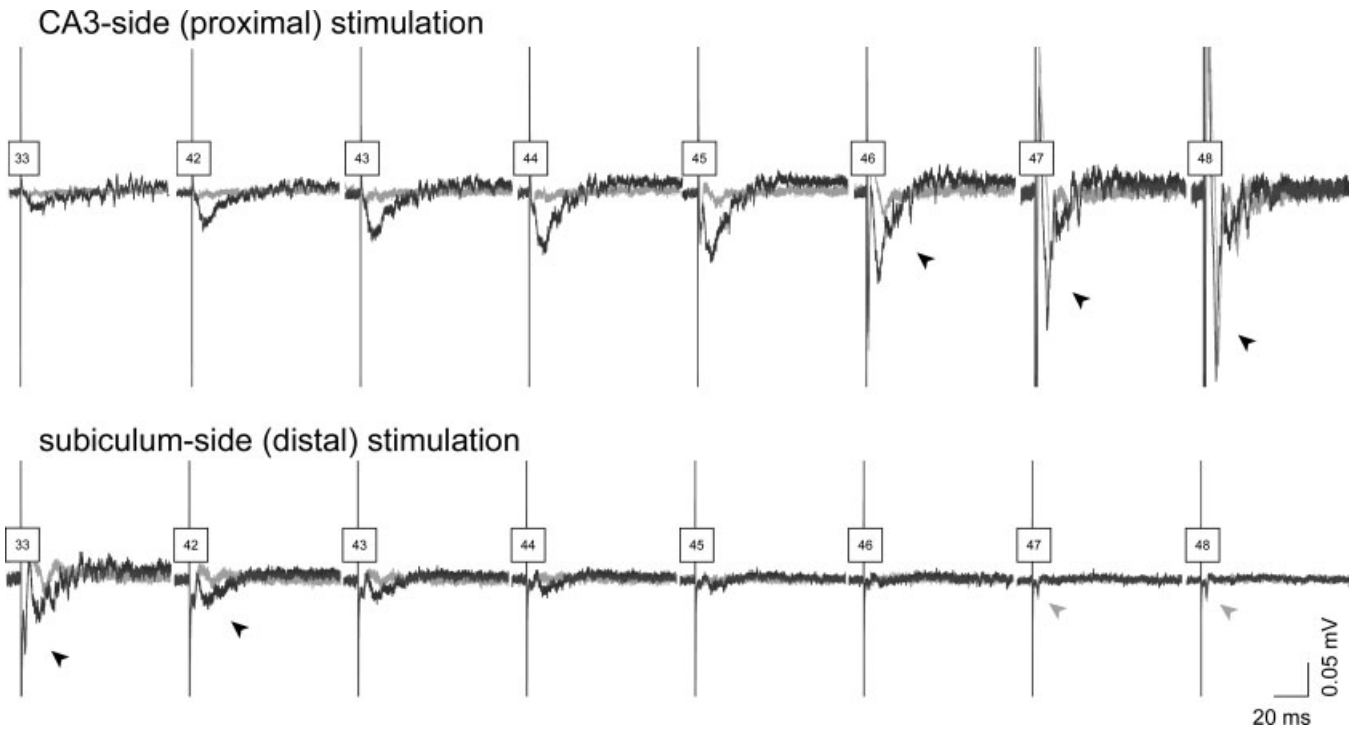

FIGURE 2. Unidirectional spread of triggered population activity along the proximo-distal axis in CA1. Top row: series of recordings from eight recording sites showing propagation (from right to left) of population events triggered by a single stimulus pulse on the CA3 (proximal) side of CA1. Black arrowheads in the right three panels point to the negative population spikes, often an initial large spike followed by later smaller spikes on a slow negativity that is a synaptic event. Numbers in the boxes associated with each trace are the channel number along the cell layer to highlight firing. Consecutive numbers are separated by 100 μm. Electrode 33 is separated from electrode 42 by 141.4 μm because it is located on a diagonal of the grid. Boxes are calibrations, illustrated again at the lower right of the figure. Black traces are recordings during disinhibition with bicuculline (50 μM). Superimposed gray traces include CNQX and CPP to identify antidromic activity. The duration of firing is clearly seen to increase as more distant recording sites are examined. Bottom row: recordings from the same set of electrodes in the same slice in response to triggering stimuli applied on the subicular (distal) side of CA1. The stimulus currents were matched to highlight the fact that the antidromic spike is large even when the synapticallly-mediated event is relatively small. Propagation is from left to right. Black arrowheads in the left two panels point to negative population spikes (as above). Gray arrowheads in the right two panels point to negative antidromic population spikes. Note the rapid decay of the evoked response revealing only the single antidromic spike at the most distant recording sites.

illustrated in Figure 3, and the regression parameters are summarized in Table 1.

One of the advantages of the grid electrode is its ability to offer coarse "depth" profiles of voltage responses. These confirmed population spikes to be from the cell layer [e.g., (Kloosterman et al., 2001; Vreugdenhil et al., 2005)]. Firing in intracellular recordings coincident with epileptiform population spiking in field potentials has also been demonstrated in numerous studies [for area CA1, examples include (Jensen and Yaari, 1997; Traynelis and Dingledine, 1988; Karnup and Stelzer, 2001)]. The late phase was a negative wave on the basal dendritic side of the cell layer, and an extracellular positivity on the apical dendritic side of the cell layer. The phase reversal was at or slightly apical to the apical edge of the cell layer. Taken together with the pharmacological resistance to NMDA and GABA-B receptor blockade, these data indicate that the late slow phase of the population event is mainly basal dendritic excitation mediated by non-NMDA receptor activation that outlasts the period of firing in CA1 pyramidal cells. We selected for measurements electrodes that were close to the cell layer because our emphasis was on cell firing, but most commonly we picked electrode sets for duration measurements that lay along the basal side of the cell to include the late phase in our measurements of total duration. Selecting electrodes in this manner (i.e., along the basal or apical side of the phase reversal for the late component) preserved our examination of population spiking without forcing us to underestimate the duration of the late phase by sampling electrodes that laid "on" the phase-reversal.

In contrast to the propagation and broadening of events that spread from the proximal side of CA1 toward the distal side, propagation of population events in the direction "backward" toward CA3 was characterized by a rapid decline in both the event amplitude and duration measures (see Figs. 2 and 3). Measured parameters had the same basic features, including the laminar appearance of the late synaptic component (Fig. 4). The distance over which we saw events spreading did not correlate with stimulus intensity.

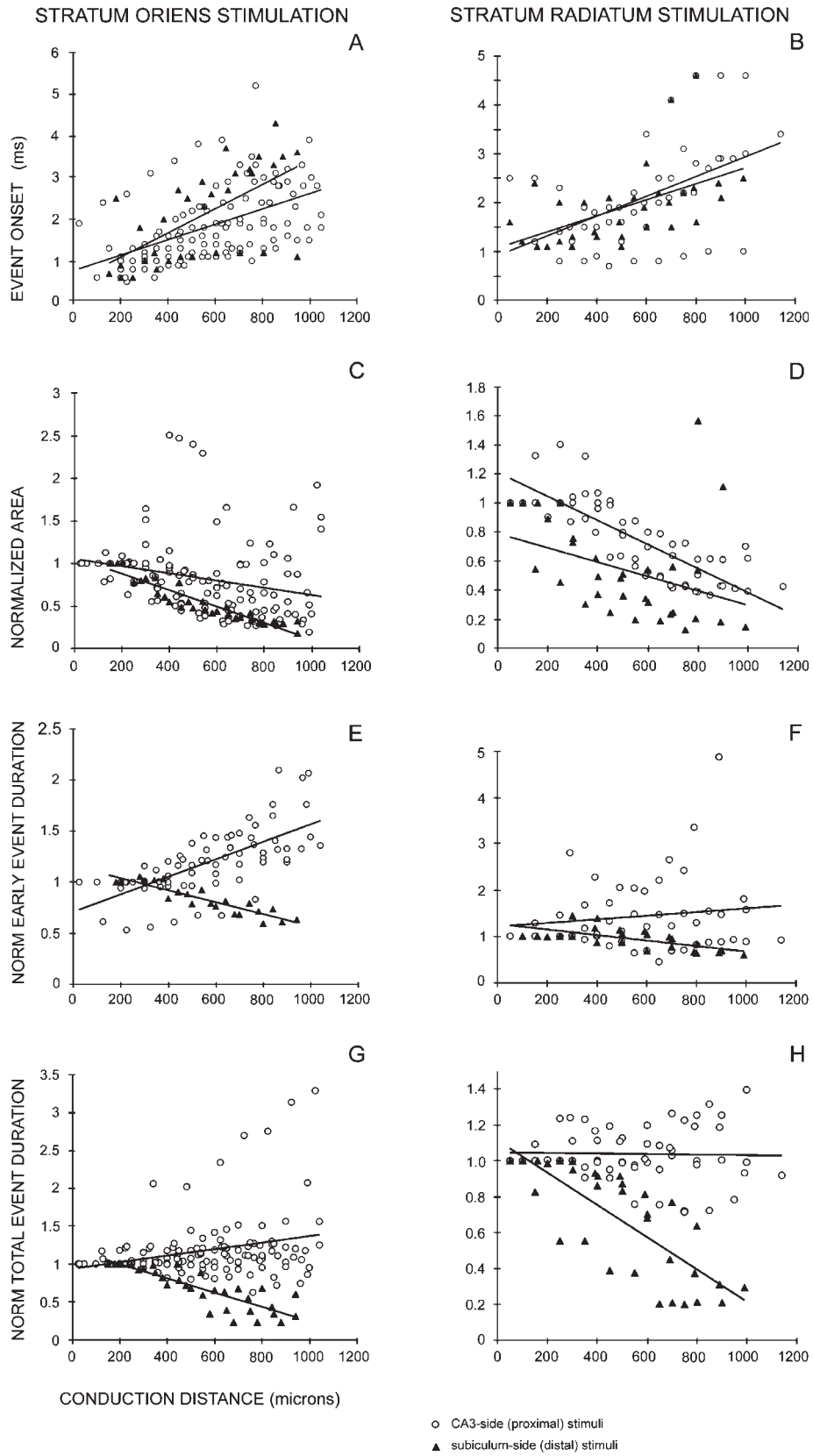

FIGURE 3. Comparison of spread and broadening in events evoked by proximal or distal stimuli applied to stratum oriens or stratum radiatum. Top row (A, B) are plots of actual event onset measures. Open circles represent data from CA3-side or proximal stimuli (stratum oriens in left column, stratum radiatum in right column), and filled triangles represent data from subicular-side or distal stimuli (stratum oriens in left column, stratum radiatum in right column). Plots contrasting normalized area (C, D), normalized early event duration (E, F), and normalized total event duration (G, H) are similarly organized. The differences in duration measures between proximal and distal stimuli are readily apparent. Event broadening is indicated by positive slopes in the duration plots and is seen only for proximal stratum oriens stimulation (open circles in plots E and G). Nondecrementing responses are seen in events triggered by stratum radiatum stimuli (open circles in plots F and H). All measures decrement rapidly for events triggered by distal stimuli. See Table 1 and text for additional details and statistical analyses.

TABLE 1.

Summary of Spread and Broadening Measures for Triggered Events in CA1 and Statistical Comparisons of Data by Stimulation Sites

		CA3-side stimulation		Subicular-side stimulation		CA3 vs. sub (same lamina)	Oriens vs. radiatum (same side)
		Stratum oriens (A)	Stratum radiatum (B)	Stratum oriens (C)	Stratum radiatum (D)		
Event onset	Slope[a]	+2.4 ± 0.2 ms/mm (N = 16 slices)	+2.3 ± 0.3 ms/mm (N = 7)	+2.9 ± 0.4 ms/mm (N = 4)	+2.1 ± 0.4 ms/mm (N = 4)		
	velocity	0.42 m/s	0.43 m/s	0.34 m/s	0.48 m/s		
Peak-to-peak amplitude	value at closest electrode	0.53 ± 0.08 mV	0.4 ± 0.13 mV	0.49 ± 0.29 mV	0.52 ± 0.23 mV		
	Slope[b] (normalized)	−1.1 ± 0.1/mm	−1.1 ± 0.1/mm	−1.1 ± 0.2/mm	−0.8 ± 0.2/mm		
Area	value at closest electrode	3.19 ± 0.31 mV μm	3.48 ± 0.77 mV μm	4.22 ± 1.99 mV μm	3.17 ± 0.73 mV μm		
	Slope[c] (normalized)	−0.6 ± 0.1/mm	−0.9 ± 0.1/mm	−1.0 ± 0.2/mm	−0.6 ± 0.2/mm		
Early duration	value at closest electrode	40.8 ± 7.4 ms	30.7 ± 6.5 ms	60.4 ± 30.9 ms	28.9 ± 3.1 ms		
	Slope[d] (normalized)	+0.8 ± 0.1/mm	+1.2 ± 0.2/mm	−0.6 ± 0.3/mm	−0.7 ± 0.2/mm	AC: 0.000 BD: 0.000	
Total duration	value at closest electrode	150.1 ± 9.5 ms	154.8 ± 7.3 ms	157.3 ± 40.3 ms	131.5 ± 36.8 ms		
	Slope[e] (normalized)	+0.4 ± 0.1/mm	+0.0 ± 0.1/mm	−1.0 ± 0.1/mm	−1.0 ± 0.1/mm	AC: 0.000 BD: 0.000	AB: 0.001 CD: NS

Stimulus intensities were adjusted such that response measures at the closest electrode to the stimulator for each stimulation site were similar. These values did not differ significantly. Statistical results are given immediately below the table. In the right 2 columns are the results of comparisons between stimulation sites: proximal vs. distal loci or oriens vs. radiatum. Graphical displays are shown in Figure 3.

Values are reported as mean ± SEM.

Blank cells in the significance columns indicate NS ($P > 0.05$).

[a,b]All slopes were significantly different from 0 ($P = 0.000$).

[c]All slopes were significantly different from 0 ($P = 0.000, 0.000, 0.000, 0.004$).

[d]All slopes were significantly different from 0 ($P = 0.000, 0.000, 0.016, 0.004$).

[e]Three slopes were significantly different from 0 ($P = 0.000$). B = NS.

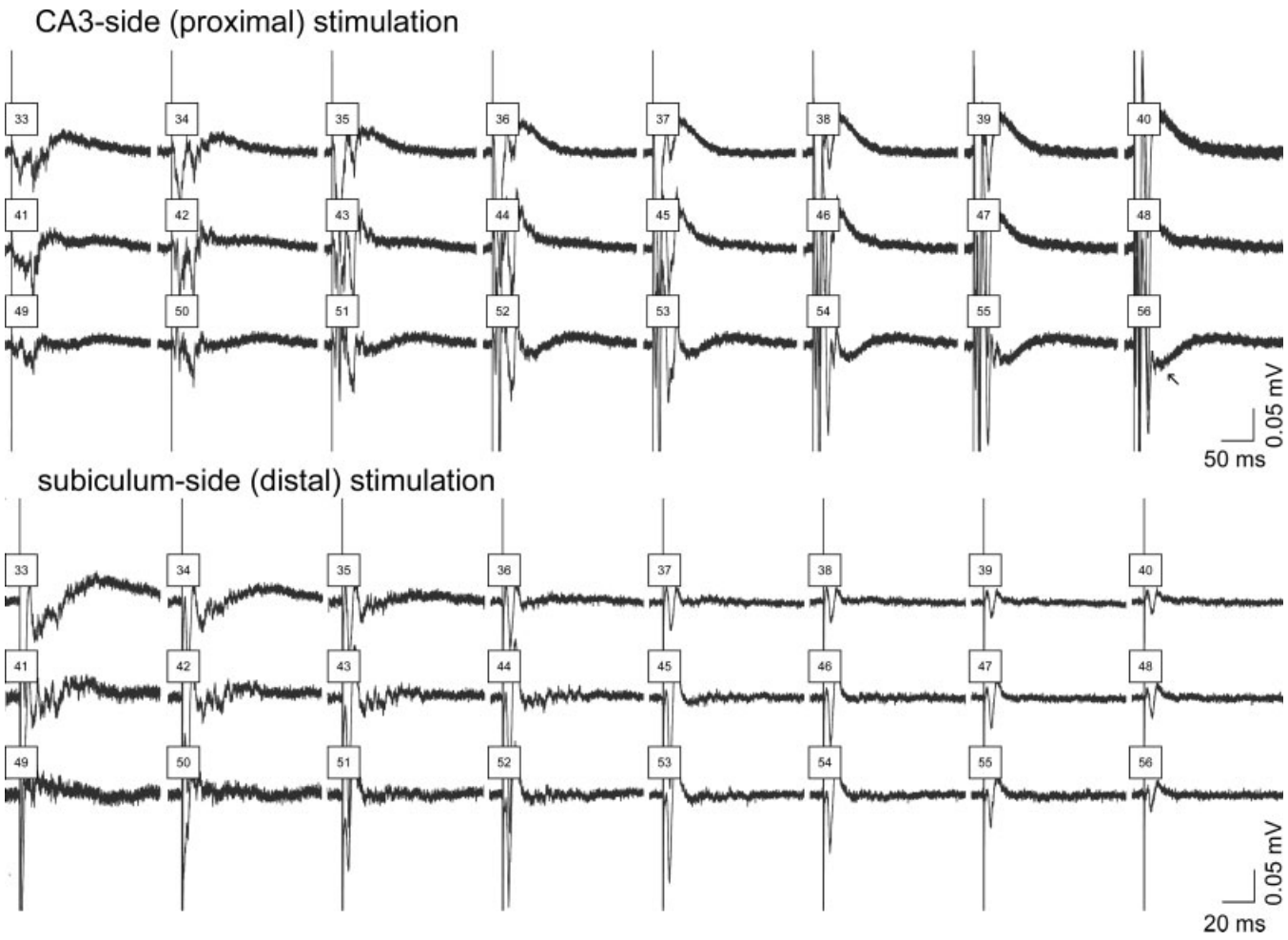

FIGURE 4. Profiles of the late slow phase following firing for forward and backward events. Each distance from the stimulating electrode is represented by a set of three recordings which were along the primary dendritic axis of the CA1 pyramidal cells. Propagation is right to left for the top panel and left to right for the bottom panel. The center row in each set is at the cell layer, the top row is 100 μm apical to this site and the bottom row is 100 μm basal to this site. The late slow phase is a positivity in apical locations and a negativity in basal locations (arrow in the rightmost set). This is the same voltage profile for events triggered by distal stimuli (bottom panel, left most set). Consecutive numbers along the row, and electrodes in each column are separated by 100 μm.

Spread

Event onsets plotted as a function of distance from the stimulating electrode were used to estimate the propagation velocity of epileptiform discharges. Propagation velocity was <0.5 m/s (500 μm/μs) irrespective of the stimulation location (Fig. 3, Table 1). Propagation was not changed by knife cuts to disconnect area CA3 or the parahippocampal areas, or by increasing potassium concentration beyond 5 mM.

We looked at the conduction velocity for antidromic population spikes evoked by proximal-side or distal-side stimulation, recorded in the presence of CNQX and either CPP or AP5 added to the perfusate that already contained bicuculline. The conduction velocity for antidromic events to the most distant electrode was 0.2–0.3 m/s when proximal stimuli were used and 0.3–0.4 m/s when distal stimuli were used. In fact, for events triggered by subicular-side stimulation, only antidromic responses were being recorded at the most distant electrodes (Figs. 2 and 4). All velocities are consistent with conduction over lightly or unmyelinated axons (Andersen et al., 2000), and do not suggest significant delays from serial cell to cell transmission.

It is important to note that antidromic responses were always single spikes and never bursts [as reported for subiculum (Stewart, 1997)] and that although some pyramidal cells were antidromically activated by subiculum-side stimulation, antidromic spikes in the presence of intact excitatory transmission did not trigger epileptiform bursts.

In three slices, we captured the spread through CA1 of spontaneous events whose origin was either uncertain or confirmed to be in CA3. In these datasets, we looked at several indicators as measures of conduction velocity. Earliest evidence of activity (leftmost line in Fig. 5) and peak of the afterdischarge (rightmost line in figure) gave conduction velocity estimates that were 0.1–0.05 m/s, whereas the maximum slope measure gave velocity measures that were consistently slower. All measures

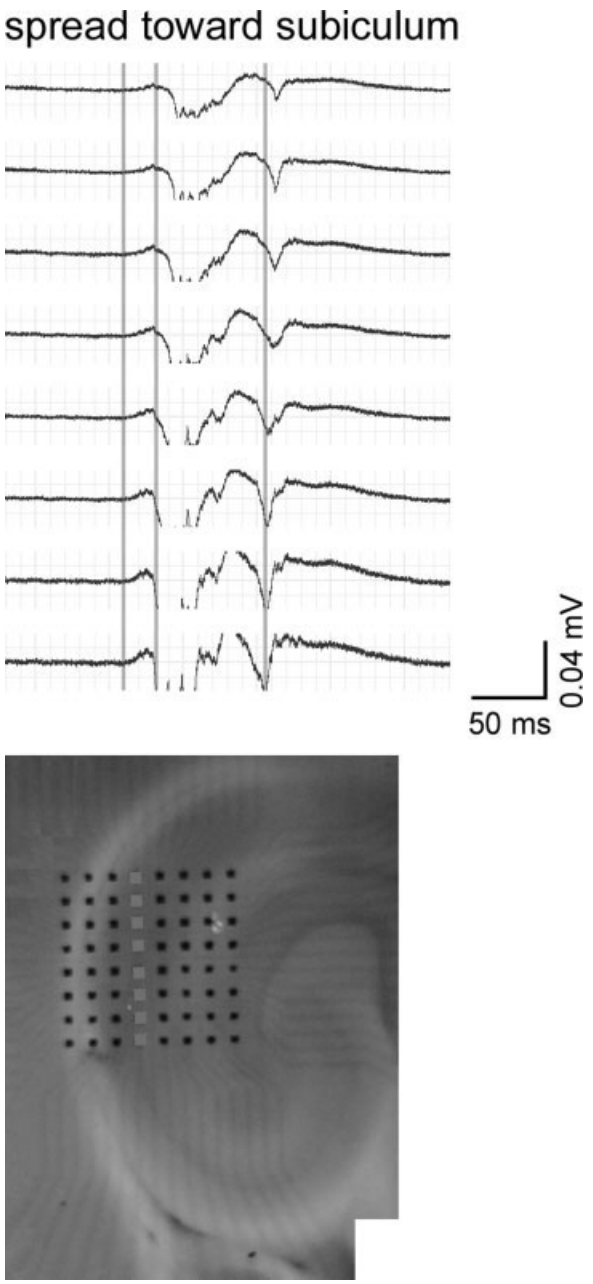

FIGURE 5. Spread of spontaneous population activity along the proximo-distal axis in CA1. Spontaneous epileptiform discharge with one clear afterdischarge spreading from near CA3 (bottom trace and lowest electrode in the image) to near subiculum (top trace and uppermost electrode in the image). Three reference lines are shown in gray. The leftmost line marks the first clear deviation from baseline evident in the most proximal recording (bottom trace). The second line from the left marks the steepest slope in the main part of the period of firing. The rightmost line marks the peak of the afterdischarge. Using each of these measures produces different estimates of conduction. Earliest activity and the peak of the afterdischarge both give values of <10 μs (about 7 μs) to propagate a distance of 700 μm for a conduction velocity of about 0.1 m/s. Using the slope marker, the conduction velocity is estimated at about half of the other estimates (0.05 m/s). At the bottom is an image of the slice with the electrode grid. The electrophysiological data are from the highlighted set of electrodes.

gave conduction velocities that were slower than the measures determined from triggered events, but evidence of firing preceding population discharges was found in some cases with intervals resembling the intervals found in triggered events.

Broadening

A feature of some networks whose members sequentially activate each other is a progressive increase in the amount of time that loci are active, as one moves further away from the site of initiation. In other words, evoked responses can "broaden."

Amplitude measures were not sensitive enough to define broadening. Increasing temporal dispersion of cell firing was expected to rapidly affect peak-to-peak amplitudes, but our area measures also declined indicating a real decrease in the number of active cells as a function of distance. As described earlier, antidromic responses were confirmed pharmacologically in some slices. The rate of decay in the amplitude measures, therefore, can be underestimates if synaptically-mediated responses are actually absent before the last electrode is reached. We consider the underestimation error to be small because the antidromic events themselves were a small fraction of the total event.

Duration measures were better for detecting and defining polysynaptic activity. Broadening was determined by measuring two durations: (a) an "early event duration" which was defined as activity between the event onset and the point of transition from firing to the late slow component, and (b) the total event duration. These measures showed striking differences depending on whether responses were triggered with proximal or distal stimuli.

Slope determinations revealed three conditions: a significant positive slope indicated that the event duration increased with distance, a nonsignificant slope (not different from 0) indicated that the event maintained its duration with distance, and a significant negative slope indicated that the event decreased in duration with distance. All events evoked by either stratum oriens or stratum radiatum stimulation on the subicular side of CA1 showed significant decreases in event duration (both early and total duration) with distance (Fig. 3), again, consistent with a rapidly shrinking population of active cells. By contrast, events evoked by proximal stimuli showed increases or stable response durations. The durations of antidromic spikes were brief enough not to introduce significant error to the early and total event duration measures for events triggered by distal stimuli.

The most sensitive measures for the polysynaptic activity in area CA1 were the duration measures which defined times during which there was firing and evidence of excitatory synaptic activity. The amplitude measures were the least sensitive because triggered events steadily decreased in amplitude even when there was propagation. The choice of onset measure depends on the experimental setup, but the point of earliest activity was the most consistent in our opinion, and, when events are triggered, onset can be confirmed by contrasting evoked

responses in the absence or presence of pharmacological blockade of excitatory transmission.

DISCUSSION

The intrinsic connectivity of CA1 is sufficient to support the generation of epileptiform events and their propagation over its proximo-distal axis. Population events triggered on the proximal side of CA1 spread across the proximo-distal extent of the subregion, but events did not spread in the reverse direction when triggered with distal (subicular-side) stimulation. Antidromic responses at the most distant recording sites were more commonly elicited by subicular-side stimuli, but such responses were not sufficient to trigger epileptiform discharges when excitatory transmission was intact. Further, based on the extent of spread in the disto-proximal direction, we estimate the local extent of CA1 intrinsic axons (excepting axonal extensions arising from projection axons) to be on the order of 300 μm, consistent with anatomical data (Lorente de No, 1934). The conduction velocity for spreading events approximated the conduction velocity for antidromic action potentials in CA1. We conclude that the unidirectional spread of population activity results from the combination of: (1) the proportionally larger axonal projection toward subiculum by CA1 cells, and (2) the fact that some local collaterals arise from these projection branches, resulting in a uniquely asymmetrical intrinsic collateral system (Fig. 6). This collateral system can be utilized for seizure spread, but its unidirectionality protects against reentrant activation of CA3, and may serve a function role in relaying activity from proximal portions of CA1 to distal portions of CA1.

Bases for the Asymmetry in CA1

While anatomical or physiological data from individual cells may or may not be representative of the majority, field potentials, especially when pharmacologically simplified from a structure such as CA1, offer considerable information about population activity. The asymmetry of the collateral system is evidenced by the unidirectional spread of epileptiform events and by the fact that antidromic responses were more commonly evoked and larger when distal stimuli were used. Interestingly, tetanic stimulation elicited similar asymmetries in the generation of gamma frequency activity in vitro (Colling et al., 1998; Stanford et al., 1998). The finding that the speed of conduction for triggered events closely resembled the speed of antidromic responses is evidence for the functional utility of the long axon collaterals. The sparseness of the CA1 connectivity is attested to by the significant decrement in event amplitude that is not simply the result of temporal dispersion of firing, and the finding that antidromic spikes evoked by distal stimuli did not recruit other cells to form a population discharge. Polysynaptic events have been reported in response to antidromic activation of what may be larger groups of cells (Crepel et al., 1997).

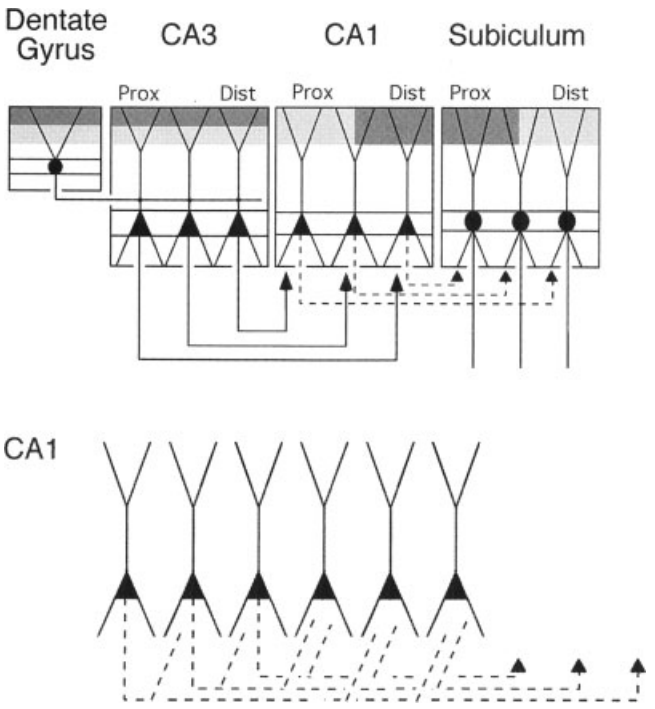

FIGURE 6. Schematic representation of CA1 pyramidal cell axonal connectivity used for the proximo-distal spread of synchronized events. Top: schematic of intrahippocampal connectivity illustrating established views of dentate to CA3. CA3 to CA1, and CA1 to subiculum connections. This figure is styled to resemble Figures 3–56 from Amaral and Lavenex (Amaral and Lavenex, 2007). Pyramidal cell bodies are represented as triangles for areas CA3 and CA1. Below: Area CA1 is highlighted to permit the added detail of ascending collaterals that contact other pyramidal cells. Possible connections with interneurons are not shown. The result is an extensive fiber system directed toward the subiculum with opportunities for rapid long-range excitation of distal CA1 cells by proximal CA1 cells, and for sequential spread of excitation over limited local collaterals.

We would argue that the asymmetric spread of activity results from asymmetrical axonal arbors. The anatomical evidence for a dense projection from CA1 to subiculum is well established (Witter and Amaral, 2004). There are examples of individual CA1 neurons with pronounced asymmetries of their axonal arbors (Finch and Babb, 1981; Knowles and Schwartzkroin, 1981; Tamamaki et al., 1987), although some cells have symmetrical axonal arbors (Finch et al., 1983). Importantly, for the development of the argument that projection collaterals contribute to the asymmetry of the intrinsic collateral system, there are several examples of CA1 pyramidal cells showing axonal extensions that reach up into stratum oriens arising from the major collaterals (Knowles and Schwartzkroin, 1981; Lorente de No, 1934). Lorente de Nó described both the local axonal arbors around individual CA1 cells (Lorente de No, 1934) (we have similar data from Golgi studies in rats, unpublished), and collaterals arising from CA1 alvear fibers that entered the "lower parts" of CA1. None of these data, however, prove that axonal processes form excitatory connections

between pyramidal cells, but Witter (Witter and Amaral, 2004) suggested that "these collaterals might be the substrate for projections from CA1 pyramidal cells to the basal dendrites of other CA1 cells." Our data support the conclusion that some of the targets are in fact pyramidal cells.

Triggered events are generated by polysynaptic and repeated excitation of pyramidal cells [see also (Crepel et al., 1997)], but the velocity of spread suggests that the earliest synaptic activity at each recorded site arises from a small number of synapses in series (possibly monosynaptic). One question that arises then is whether the unidirectionality of the Schaffer collateral system contributes to the asymmetry we observe. Stimuli applied to either stratum radiatum or stratum oriens were similarly effective for triggering spreading population events. Events triggered by stratum oriens stimuli, even when the stimulating electrodes were placed well inside CA1, showed broadening with distance, and suggest that the most sustained and highest levels of excitation are elicited by stratum oriens stimulation. Stimuli applied to the subicular-side of CA1 might be expected to have an equivalent excitatory priming effect because these stimuli activate projection axons, although such activation was found to be primarily antidromic. The absence of such an excitatory priming effect in the reverse direction can be explained by the asymmetry of the axonal arbors (Fig. 6). A decreasing number of axons as one move toward proximal CA1 would lead to a progressive decline of any excitatory priming effect as a function of distance along the disto-proximal axis. A similar decline in excitatory priming will occur when Schaffer collaterals are activated, and therefore would be expected to promote activity in a steadily shrinking population of pyramidal cells. Neither the antidromic activation of CA1 cells, nor Schaffer collateral activation can account for the sustained polysynaptic activity we observed.

Spread and Broadening

In biological studies, we have seen spread in both directions along a proximo-distal axis in subiculum (Harris and Stewart, 2001a) and EC (Stewart, 1999), although there are some differences in activity depending on the direction of spread (Funahashi and Stewart, 1998). Spread is also reported to be bidirectional in neocortex (Chervin and Connors, 1986; Gutnick and Wadman, 1986). The rates of spread in different cortical regions vary somewhat. Nondecrementing (and sometimes broadening) population events spread through area CA3 at 0.15 m/s CA3 (Miles et al., 1988). This was similar to the rates reported for neocortex, 0.13–0.19 m/s neocortex (Golomb and Amitai, 1997), and disinhibited hippocampal neurons cultured on a line, 0.1 m/s (Feinerman et al., 2005). Lower rates were reported in other studies of neocortex, 0.074 m/s (Pinto et al., 2005), and in subiculum, 0.04 m/s subiculum (Harris and Stewart, 2001a). These rates are all lower than the reported conduction velocity for unmyelinated CA3 axons [longitudinal association fibers: 0.39 m/s, Schaffer collaterals: 0.25 m/s (Andersen et al., 2000)].

Uniformly connected cells in a distributed network model show features of the forward spreading in CA1 or activity seen in other hippocampal formation areas whose intrinsic connectivity appears symmetrical. Among the most significant parameters associated with the rate for propagation of a population event are the connectivity properties within local clusters or modules of neurons and between modules, but these parameters govern spread generally. The intramodule connectivity establishes a threshold to activate groups of cells (Beggs and Plenz, 2003; Lytton et al., 2005), and as one module excites an adjacent module, the duration of activity increases, a process we refer to as broadening.

Broadening is seen as a negative consequence of population events propagating in a neuronal network (Traub et al., 1999; Vogels et al., 2005). The excitatory and inhibitory parameter sets are difficult to configure such that sets of active neurons (synfire packets) do not recruit larger numbers of cells, or that individual cells do not sustain activity, as events propagate [e.g., (Lytton et al., 2005; Vogels and Abbott, 2005)]. Model networks (CA3 and CA1) change from normal low rates of activity to seizing to bursting as the number of long-distance connections is increased (Netoff et al., 2004). The extreme example of this inappropriate recruitment [epileptic chain reaction, neuronal avalanche, synfire chain explosion; reviewed in (Traub et al., 1999; Vogels et al., 2005)] is the finding that activation of a single CA3 pyramidal cell can synchronize the entire population (Miles and Wong, 1983). Such expansion in time of neuronal activity, or a dissipation of activity (synfire chain failure) means that the packets themselves cannot function as faithful relay mechanisms (Vogels et al., 2005).

In biological preparations, inhibitory circuits are clearly critical for preventing the inappropriate recruitment of neurons in modules as population discharges spread successively through a series of such modules that comprise a brain area. Although the various types of inhibitory cells, their principal modes of activation, firing, and targets are all quite well defined [e.g., (Buhl and Whittington, 2007)], there are no data to suggest that there are quantitative differences in the numbers of inhibitory cells, the types of inhibitory cells, or the strength of inhibition on pyramidal cells as a function of location along the proximo-distal axis. In area CA1, the suppression of inhibition was shown to be critical for the spread of epileptiform events out of the area and into subiculum (Benini and Avoli, 2005). By contrast, Pinto et al. (2005) showed that propagation in the neocortex did not depend on inhibition; inhibition determined event duration. Broadening in disinhibited preparations is contrasted with the more stable sharp wave (Buzsaki, 1986) spreading through hippocampal formation areas. These normally-occurring synchronous population events do not show broadening as they spread. Rather, an interesting by-product of the functioning inhibitory network is the period of gamma frequency activity that trails the propagating sharp wave [e.g., (Ylinen et al., 1995; Funahashi and Stewart, 1998)] and can contribute to long-range synchrony [reviewed in (Traub et al., 1999); see also (Csicsvari et al., 2003; Funahashi and Stewart, 1998)].

Functional Implications

What purpose might the asymmetrical collateral system serve? This organization is certainly an additional safeguard against reentrant activation of area CA3, perhaps the most seizure-prone region in the brain. Seizure "prevention" is not, however, likely to be the natural function of a brain region's collateral system. An interesting and functional possibility comes from the role of area CA1 in spatial information processing.

The "place" signal found in CA1 pyramidal cells [reviewed in (O'Keefe, 2007)] is derived from a spatial signal in "grid cells" of the medial EC (Hafting et al., 2005; Sargolini et al., 2006). Spatial information comes to CA1 from medial and not lateral EC (Knierim et al., 2006). The medial EC projects to proximal CA1 whereas the lateral EC projects to distal CA1 (Steward, 1976), and these inputs are segregated. One would predict, therefore, that spatial firing in CA1 (place cell activity) would be found in the proximal, but not distal CA1. The available physiological data suggest that this prediction is wrong and that place cells exist over the entire proximo-distal extent of CA1. We suggest that the unidirectional intrinsic collateral system in CA1 functions as a relay of spatial or other signals from proximal CA1 neurons to distal CA1 neurons.

Acknowledgments

We thank Dr. Frank Schottler for many of the Microsoft EXCEL macros used to read and analyze the MED64 Conductor files.

REFERENCES

Amaral D, Lavenex P. 2007. Hippocampal neuroanatomy. In: Andersen P, Morris R, Amaral D, Bliss T, O'Keefe J, editors. The Hippocampus Book, Chapter 3. Oxford, New York: Oxford University Press. pp 37–114.

Andersen P, Soleng AF, Raastad M. 2000. The hippocampal lamella hypothesis revisited. Brain Res 886:165–171.

Beggs JM, Plenz D. 2003. Neuronal avalanches in neocortical circuits. J Neurosci 23:11167–11177.

Benini R, Avoli M. 2005. Rat subicular networks gate hippocampal output activity in an in vitro model of limbic seizures. J Physiol 566 (Part 3):885–900.

Buhl E, Whittington MA. 2007. Local circuits. In: Andersen P, Morris R, Amaral D, Bliss T, O'Keefe J, editors. The Hippocampus Book, Chapter 8. Oxford, New York: Oxford University Press. pp 297–319.

Buzsaki G. 1986. Hippocampal sharp waves: Their origin and significance. Brain Res 398:242–252.

Chervin RD, Connors BW. 1986. Lateral propagation of synchronized paroxysmal discharges in the disinhibited neocortex. Soc Neurosci Abstr 12:350 (#94.7).

Colling SB, Stanford IM, Traub RD, Jefferys JG. 1998. Limbic gamma rhythms. I. Phase-locked oscillations in hippocampal CA1 and subiculum J Neurophysiol 80:155–161.

Crepel V, Khazipov R, Ben-Ari Y. 1997. Blocking GABA(A) inhibition reveals AMPA- and NMDA-receptor-mediated polysynaptic responses in the CA1 region of the rat hippocampus. J Neurophysiol 77:2071–2082.

Csicsvari J, Jamieson B, Wise KD, Buzsaki G. 2003. Mechanisms of gamma oscillations in the hippocampus of the behaving rat. Neuron 37:311–322.

Deuchars J, Thomson AM. 1996. CA1 pyramid-pyramid connections in rat hippocampus in vitro: Dual intracellular recordings with biocytin filling. Neuroscience 74:1009–1018.

Feinerman O, Segal M, Moses E. 2005. Signal propagation along unidimensional neuronal networks. J Neurophysiol 94:3406–3416.

Finch DM, Babb TL. 1981. Demonstration of caudally directed hippocampal efferents in the rat by intracellular injection of horseradish peroxidase. Brain Res 214:405–410.

Finch DM, Nowlin NL, Babb TL. 1983. Demonstration of axonal projections of neurons in the rat hippocampus and subiculum by intracellular injection of HRP. Brain Res 271:201–216.

Funahashi M, Stewart M. 1997. Presubicular and parasubicular cortical neurons of the rat: Functional separation of deep and superficial neurons in vitro. J Physiol 501 (Part 2):387–403.

Funahashi M, Stewart M. 1998. Properties of gamma-frequency oscillations initiated by propagating population bursts in retrohippocampal regions of rat brain slices. J Physiol 510 (Part 1):191–208.

Funahashi M, Harris E, Stewart M. 1999. Re-entrant activity in a presubiculum-subiculum circuit generates epileptiform activity in vitro. Brain Res 849:139–146.

Golomb D, Amitai Y. 1997. Propagating neuronal discharges in neocortical slices: Computational and experimental study. J Neurophysiol 78:1199–1211.

Gutnick MJ, Wadman WJ. 1986. Intrinsic neuronal connectivity in neocortical brain slices as revealed by non-uniform propagation of paroxysmal discharges. Soc Neurosci Abstr 12:349 (#94.6).

Hafting T, Fyhn M, Molden S, Moser MB, Moser EI. 2005. Microstructure of a spatial map in the entorhinal cortex. Nature 436:801–806.

Harris E, Stewart M. 2001a. Intrinsic connectivity of the rat subiculum. II. Properties of synchronous spontaneous activity and a demonstration of multiple generator regions. J Comp Neurol 435:506–518.

Harris E, Stewart M. 2001b. Propagation of synchronous epileptiform events from subiculum backward into area CA1 of rat brain slices. Brain Res 895:41–49.

Harris E, Witter MP, Weinstein G, Stewart M. 2001. Intrinsic connectivity of the rat subiculum. I. Dendritic morphology and patterns of axonal arborization by pyramidal neurons. J Comp Neurol 435:490–505.

Heinemann U. 1987. Basic mechanisms of epilepsy. In: Halliday AM, Butler S, Paul R, editors. A textbook of Clinical Neurophysiology. Chichester, New York: Wiley. pp 497–534.

Jensen MS, Yaari Y. 1997. Role of intrinsic burst firing, potassium accumulation, and electrical coupling in the elevated potassium model of hippocampal epilepsy. J Neurophysiol 77:1224–1233.

Karnup S, Stelzer A. 2001. Seizure-like activity in the disinhibited CA1 minislice of adult guinea-pigs. J Physiol 532 (Part 3):713–730.

Kloosterman F, Peloquin P, Leung LS. 2001. Apical and basal orthodromic population spikes in hippocampal CA1 in vivo show different origins and patterns of propagation. J Neurophysiol 86:2435–2444.

Knierim JJ, Lee I, Hargreaves EL. 2006. Hippocampal place cells: Parallel input streams, subregional processing, and implications for episodic memory. Hippocampus 16:755–764.

Knowles WD, Schwartzkroin PA. 1981. Axonal ramifications of hippocampal Ca1 pyramidal cells. J Neurosci 1:1236–1241.

Kunitake A, Kunitake T, Stewart M. 2004. Differential modulation by carbachol of four separate excitatory afferent systems to the rat subiculum in vitro. Hippocampus 14:986–999.

Li XG, Somogyi P, Ylinen A, Buzsaki G. 1994. The hippocampal CA3 network: An in vivo intracellular labeling study. J Comp Neurol 339:181–208.

Lorente de No R. 1934. Studies on the structure of the cerebral cortex. II. Continuation of the study of the Ammonic system. J Psychol Neurol 46:113–177.

Lytton WW, Orman R, Stewart M. 2005. Computer simulation of epilepsy: Implications for seizure spread and behavioral dysfunction. Epilepsy Behav 7:336–344.

Miles R, Wong RK. 1983. Single neurones can initiate synchronized population discharge in the hippocampus. Nature 306:371–373.

Miles R, Traub RD, Wong RK. 1988. Spread of synchronous firing in longitudinal slices from the CA3 region of the hippocampus. J Neurophysiol 60:1481–1496.

Netoff TI, Clewley R, Arno S, Keck T, White JA. 2004. Epilepsy in small-world networks. J Neurosci 24:8075–8083.

O'Keefe J. 2007. Hippocampal neurophysiology in the behaving animal. In: Andersen P, Morris R, Amaral D, Bliss ST, O'Keefe J, editors. The Hippocampus Book, Chapter 11. Oxford, New York: Oxford University Press. pp 475–548.

Paxinos G, Watson C. 1998. The Rat Brain in Stereotaxic Coordinates. San Diego: Academic Press. xxvi p. [237] p. of plates p.

Pinto DJ, Patrick SL, Huang WC, Connors BW. 2005. Initiation, propagation, and termination of epileptiform activity in rodent neocortex in vitro involve distinct mechanisms. J Neurosci 25:8131–8140.

Sargolini F, Fyhn M, Hafting T, McNaughton BL, Witter MP, Moser MB, Moser EI. 2006. Conjunctive representation of position, direction, and velocity in entorhinal cortex. Science 312:758–762.

Spruston N, McBain C. 2007. Structural and functional properties of hippocampal neurons. In: Andersen P, Morris R, Amaral D, Bliss T, O'Keefe J, editors. The Hippocampus Book, Chapter 5. Oxford, New York: Oxford University Press. pp 133–201.

Stanford IM, Traub RD, Jefferys JG. 1998. Limbic gamma rhythms. II. Synaptic and intrinsic mechanisms underlying spike doublets in oscillating subicular neurons. J Neurophysiol 80:162–171.

Steward O. 1976. Topographic organization of the projections from the entorhinal area to the hippocampal formation of the rat. J Comp Neurol 167:285–314.

Stewart M. 1997. Antidromic and orthodromic responses by subicular neurons in rat brain slices. Brain Res 769:71–85.

Stewart M. 1999. Columnar activity supports propagation of population bursts in slices of rat entorhinal cortex. Brain Res 830:274–284.

Tamamaki N, Abe K, Nojyo Y. 1987. Columnar organization in the subiculum formed by axon branches originating from single CA1 pyramidal neurons in the rat hippocampus. Brain Res 412:156–160.

Traub RD, Jefferys JGR, Whittington MA. 1999. Fast Oscillations in Cortical Circuits. Cambridge, Mass: MIT Press. xviii,324 p.

Traynelis SF, Dingledine R. 1988. Potassium-induced spontaneous electrographic seizures in the rat hippocampal slice. J Neurophysiol 59:259–276.

Vogels TP, Abbott LF. 2005. Signal propagation and logic gating in networks of integrate-and-fire neurons. J Neurosci 25:10786–10795.

Vogels TP, Rajan K, Abbott LF. 2005. Neural network dynamics. Annu Rev Neurosci 28:357–376.

Vreugdenhil M, Bracci E, Jefferys JG. 2005. Layer-specific pyramidal cell oscillations evoked by tetanic stimulation in the rat hippocampal area CA1 in vitro and in vivo. J Physiol 562 (Part 1):149–164.

Witter MP, Amaral DG. 2004. Hippocampal formation. In: Paxinos G, editor. The Rat Nervous System, 3rd ed. San Diego: Elsevier Academic Press. Chapter 21. pp 635–704.

Ylinen A, Bragin A, Nadasdy Z, Jando G, Szabo I, Sik A, Buzsaki G. 1995. Sharp wave-associated high-frequency oscillation (200 Hz) in the intact hippocampus: Network and intracellular mechanisms. J Neurosci 15 (Part 1):30–46.